April 2008

Structure-Function Analysis of Porcine Circovirus 2 (PCV2) VP3

Jill Marie Goldstein
Worcester Polytechnic Institute

Jonathan Paul Bourque
Worcester Polytechnic Institute

Project Code: DEH DH01

DEH DH07

CLONING AND STRUCTURE-FUNCTION ANALYSIS OF PORCINE CIRCOVIRUS 2 VP3

A Major Qualifying Project:

submitted to the Faculty

of the

WORCESTER POLYTECHNIC INSTITUTE

in partial fulfillment of the requirements for the

Degree of Bachelor of Science

by

_____

Jonathan Bourque

_____

Jill Goldstein

Date: April 24, 2008

Approved:

_____

Professor Destin W. Heilman, Major Advisor

_____

Professor Kristin K. Wobbe, Co-Advisor

(Keywords)
1. Porcine Circovirus
2. Apoptin
3. Localization

Abstract

Porcine Circovirus 2 (PCV2) is in the same family as Chicken Anemia Virus (CAV). CAV Viral Protein 3 (VP3) engages in cell-type specific localization, exhibiting nuclear localization in transformed cells and cytoplasmic localization in primary cells. CAV VP3 (Apoptin) interacts with the Anaphase Promoting Complex (APC) leading to the induction of apoptosis specifically within transformed cells. This study examined the properties of PCV2 a VP3 and PCV2b VP3 in relation to those of Apoptin. Analysis of PCV2 VP3 was conducted by performing an alignment of the PCV2a VP3, PCV2b VP3 and CAV VP3 genomes, which indicates a level of homology among the proteins. The gene of interest was cloned into the eGFP vector and expressed in H1299 and MRC5 cells. Expression of this protein indicates cytoplasmic localization within both primary and transformed cells. This localization pattern differs from that of CAV VP3, yet both proteins are involved in the induction of apoptosis, therefore indicating that nuclear localization may not be required for PCV2 VP3 activity. Further analysis should investigate the mechanism of action of PCV2 VP3 in relation to its localization, multimerization capabilities and its molecular target.

Acknowledgements

We would like to thank Professor Destin W. Heilman, our Major Advisor, for allowing us to conduct research in his laboratory (WPI Department of Chemistry and Biochemistry; Worcester, MA). His guidance and assistance throughout the course of our project have been invaluable. Additionally, we would like to thank Professor Kristin K. Wobbe, our Co-Advisor, for her assistance in coordinating our project work. We would also like to thank Professor José Teodoro for the use of his laboratory and assistance in performing transfections and localization analysis (McGill University Cancer Canter; Montreal, Quebec, Canada).

Table of Contents

Tables

Figures

1 Background

1.1 Post-Weaning Multisystemic Wasting Syndrome (PMWS)

First identified in Canada in the early 1900s, Post-Weaning Multisystemic Wasting Syndrome (PMWS) has developed into a major concern for the swine industry, generally affecting pigs between 5-18 weeks of age. Porcine Circovirus (PCV) is the causative agent of PMWS, in which affected pigs exhibit symptoms of weight loss and illnesses associated with the digestive and respiratory tracts (12). Additionally, they experience severe neurological disorders, lesions on their internal organs, dermatitis and often death.

There are two serotypes of porcine circovirus, PCV1 and PCV2, which are distinguished by their response to different antibodies. Of these, only PCV2 is pathogenic in pigs. Further investigation of PCV2 has revealed that there are two important isoforms, PCV2a and PCV2b, the latter of which was recently discovered in Canada at the same time as an increase in the mortality rates and infection rates of the disease (4, 5).

1.2 Porcine Circovirus (PCV)

PCV is composed of an icosohedral protein capsid and a single stranded circular DNA genome of approximately 1.7kb. The virus particle is approximately 17nm in diameter and is non-enveloped. As displayed in Figure 1, the PCV genome contains three functional open reading frames (ORF) which have been termed cap gene, rep gene, and ORF 3 (12).

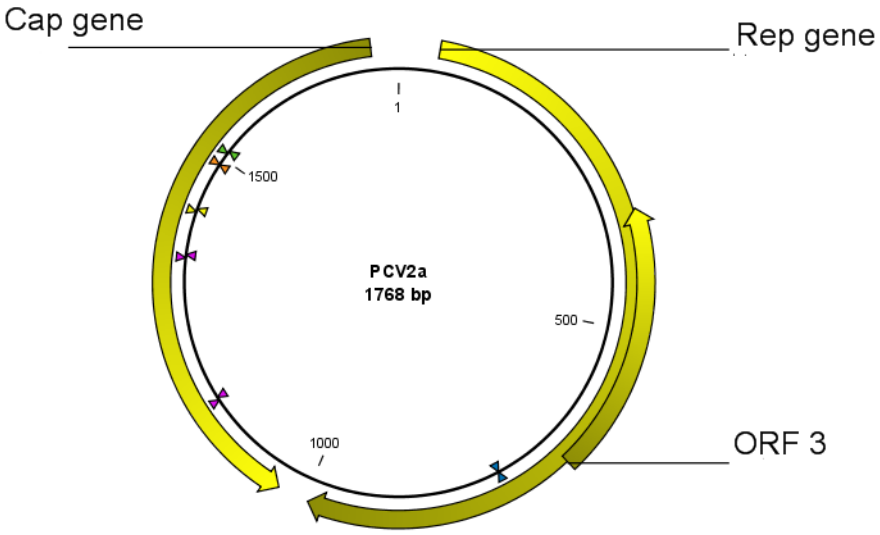

Figure 1. The Circular Genome of PCV2. The genome contains three open reading frames: Cap gene, Rep gene, and ORF 3.

Cap gene (702bp) is responsible for producing the protein capsid. The Rep gene (945bp) can be transcribed into two mRNA transcripts by alternative splicing mechanisms (1). These transcripts produce two different replicase proteins, Rep and Rep', which associate with each other in the cell. Upon association, the replicase protein complex binds to a hairpin structure at the origin of replication to initiate replication of the viral DNA (13, 21). Both the rep and cap genes are required for the production of viral particles, but ORF3 is not (10). ORF3 (315bp) plays an important role in virus induced apoptosis, which allows new viruses to exit the host cell and continue to infect other target cells. It has been shown that the product of ORF3, Viral Protein 3 (VP3), is necessary for viral pathogenesis (11).

Between PCV2a and PCV2b, the cap gene varies at 17 residues and the rep gene varies at 3 residues. However, these differences still result in viruses capable of replicating and producing antigenically indistinguishable capsids. It seems that the answer to these differences may lie in

VP3, as the ability to induce apoptosis in varied cell types is a logical mechanism for wasting in PMWS experienced by pigs infected with PCV2.

1.3 CAV VP3 (Apoptin)

It has been determined that ORF 3 in PCV2, which codes for the product VP3, is required for viral pathogenesis (11). Another virus known as Chicken Anemia Virus (CAV) also belongs to the *Circovidae* family and shares a large amount of homology with PCV2. CAV VP3, more commonly known as Apoptin, is also homologous to PCV2 VP3 (9, 14). Since little is known about VP3 in PCV2, the analysis of Apoptin may shed light on its function. Interestingly, Apoptin can selectively induce apoptosis within a cancerous cell but not within a normal primary cell, indicating the presence of a mechanism for transformed cell-specific activities (9).

In primary cells, Apoptin typically localizes in the cytoplasm with a filamentous pattern (19). By contrast, Apoptin localizes in the nucleus within transformed cells, signifying that the protein is regulated by nuclear trafficking (2,7). As a result, the sub-cellular localization patterns of Apoptin reflect the fate of the cell with regard to apoptosis. Further analysis of the protein has shown that shuttling activity of Apoptin in and out of the nucleus can influence apoptosis and the solubility of the protein in cancerous cells (9).

A factor crucial to determining the specific localization pattern of Apoptin is the presence of a Nuclear Export Sequence (NES) and a Nuclear Localization Sequence (NLS). These sequences allow the protein to bind transport receptors, which facilitate passage through the nuclear pore complex. These receptors can be subdivided into two categories: exportins, which are involved in nuclear export, and importins, which are involved with nuclear localization. When bound with GTP, the GTPase Ran binds an exportin that subsequently binds the NES of the protein. This complex dissociates in the cytoplasm in the presence of RanGAP and Ran-

binding protein 1(RanBP1). Conversely, when an NLS binds a transport receptor in the cytoplasm, it is transported into the nucleus where the receptor binds RanGTP. This binding causes the dissociation of the receptor-NLS complex, thus preventing the reverse reaction (16).

The NES consists of ten amino acids (37 to 46) at the N-terminal end of Apoptin that is crucial in shuttling the protein to the cytoplasm of primary cells. The exportin believed to be involved in the cytoplasmic localization of Apoptin is CRM1, which is specific for NES regions abundant in leucine residues (6). If leucine-44 and leucine-46 of the NES are mutated to alanines, Apoptin will localize in the nucleus of primary cells rather than in the cytoplasm. However, this mutation does not lead to apoptosis in transfected primary or cancer cells, indicating that the sub-cellular localization of Apoptin is not sufficient to induce cell death (9). The NLS consists of amino acid residues 70 to 121 at the C terminal end of Apoptin. The NLS contains two domains rich in lysine and arginine that are used to facilitate nuclear localization. Although the mechanism is still unclear, both the NES and NLS play an important role in facilitating sub-cellular localization of Apoptin within primary and transformed cells (9). Interestingly, the expression of several transport receptors is up-regulated in certain forms of cancer (20). Once in the nucleus of a transformed cell, Apoptin can selectively induce apoptosis by interacting with the Anaphase Promoting Complex (APC).

1.4 VP3-Induced Apoptosis

After passing through a cellular checkpoint, a mitotic cell transitions from metaphase to anaphase, in which an elaborate series of spindle fibers and microtubules separates the sister chromatids to opposite poles of the cell. The APC cyclosome plays a crucial role in regulating this transition into mitosis (15). As one of the larger protein complexes within the eukaryotic

cell (4 MDa), APC consists of over 13 subunits and functions as an E3 ubiquitin ligase that targets specific proteins for degradation (17).

The APC signals for the destruction of securin, the inhibitory portion of the separase enzyme involved in initiating anaphase, through ubiquitination (9). At the start of anaphase, separase binds to the cohesin complexes that connect the sister chromatids, dissolves them, and allows the chromatids to separate (19). The APC is also responsible for ubiquitinating a number of cyclins in order to regulate them at other points in the cell cycle. For example, the APC regulates the SCF E3 ligase by ubiquitination of two different subunits. This ubiquitination and subsequent degradation prevents unscheduled entry into S phase (8). Additionally, evidence such as active cytoplasmic APC in neurons, suggests that it plays additional roles in the cell (7).

Although it is currently unknown how the interaction of Apoptin with the APC leads to apoptosis, the mechanism functions via an intrinsic pathway. This pathway is activated through mitochondrial damage involving a collection of caspases, or cystine proteases. Cytochrome *c* is released by the mitochondria and is involved in the cleavage of the pre-initiator polypeptide. This cleavage results in the formation of an active initiator caspase, triggering a series of effector caspases and eventual apoptosis (3).

1.5 PCV2 VP3 Mechanism of Action

Little information has been published on the mechanism by which PCV2 is regulated or how it induces apoptosis. Using a yeast 2 hybrid system, one study has shown that VP3 interacts with porcine P53 induced RING-H2, pPirh2. Out of ten positive interactions, five corresponded to a homolog of human-Pirh2. Porcine Pirh2 acts as an ubiquitin E3 ligase specifically binding and ubiquitinating P53. This leads to degradation of P53, thus moderating its levels in healthy

cells. According to this study, VP3 binds the site on pPirh2 which usually binds P53. This could result in excess P53, which then would lead to the induction of apoptosis (18).

The sub-cellular localization patterns of Apoptin are believed to be involved in transformed cell-specific apoptosis. However, the localization patterns of PCV2a VP3 and PCV2b VP3 in both primary and transformed cells have yet to be determined. By evaluating the level of homology among PCV2a VP3, PCV2b VP3 and Apoptin, we will be able to characterize the differences among the proteins at an amino acid level. Additionally, this study will serve to clone both PCV2a VP3 and PCV2b VP3 in order to analyze their sub-cellular localization patterns within both transformed and primary cells. This analysis may provide valuable insight on the similarities between the characteristics of PCV2 VP3 and Apoptin and could enhance our understanding of cellular transformation.

2 Materials and Methods

Sequence Analysis

Sequence alignments for PCV2a VP3, PCV2b VP3 and Apoptin were performed using CLC Free Workbench 4.0.2 developed by CLC bio A/S. Visual analysis of functional homology among PCV2a VP3, PCV2b VP3, and CAV VP3 was performed using data from clustal alignment.

Reconstruction of VP3

The initial PCV2a and PCV2b clones had been linearized within the VP3 coding region. In order to examine the properties of both isoforms of VP3, we required the wild-type genes. These full-length genes for PCV2a VP3 and PCV2b VP3 were reconstructed by PCR using *Taq* polymerase, Standard *Taq* Buffer, 10mM dNTP and primers at a concentration of 25µM. The primers in Tables 1 and 2 were designed to amplify the 5' fragment and the 3' fragment of ORF 3 from the pCR Blunt clone. Restriction sites for EcoR1 and BamH1 were included in the terminal primers on the 5' and 3' ends, respectively. Amplification of the VP3 fragments was achieved through the following temperature protocol: Initial denaturing at 95° for 4 minutes; 30 cycles of amplification (95° for 30 s, 55° for 30 s, 72° for 1 min) followed by a final extension at 72° for 5 min. A 20-fold and a 100-fold dilution of each sample were prepared. Both 20-fold dilutions and both 100-fold dilutions were combined and allowed to anneal at 90° for 7 min. The same PCR temperature protocol was used to amplify the full-length PCV2a VP3 and PCV2b VP3 genes using the 5' F and 3' R primers.

Table 1: PCR Amplification Primers for PCV2a VP3

3' Fragment Reverse	GCGGATCCAATTACTTATTGAATGTG
3' Fragment Forward	CTCACTTTCAAAAGTTCAGCCAGCCC
5' Fragment Reverse	GCGGGCTGGCTGAACTTTTGAAAGTG
5' Fragment Forward	CGAATTCAATGGTAACCATCCCACCACTT

Table 2: PCR Amplification Primers for PCV2b VP3

3' Fragment Reverse	CGAATTCAATGGTAACCATCCCACCACTT
3' Fragment Forward	GTTTGTCAGAAATTTCCGCGGGCTGGCTGAACTTTTGAAA
5' Fragment Reverse	AAAAGTTCAGCCAGCCCGCGGAAATTTCTGACAAACGTTA
5' Fragment Forward	CGGATCCAATTACTGATTGAGTGTGGAGCT

Cloning of VP3 Gene into eGFP Vector

Wild type PCV2a VP3 and PCV2b VP3 were sub-cloned into pGEM T vector using Promega kit #A3600. pGem T-VP3 and eGFP-C1 were both cut with BamH1 and EcoR1 restriction enzymes in Buffer E. The full-length VP3 genes were gel purified using Promega kit #7170. The eGFP vector and purified VP3 inserts were allowed to ligate for 1 hour at room temperature using ligase buffer from Promega of the following composition: 300 mM Tris-HCl (pH 7.8), 100 mM $MgCl_2$, 100 mM DTT and 10 mM ATP. These constructs were cloned into *E. Coli* DH5α cells and were confirmed by restriction digest analysis and DNA sequencing. The eGFP-VP3 constructs were scaled up via Midipreperation using the following solutions: I. (pH 8.0) 50 mM glucose, 25 mM Tris-HCl, 10 mM EDTA; II. 0.2 M NaOH, 1% SDS; III. (pH 4.92) 5 M acetate buffer.

Transfection into H1299 and MRC-5 Cells

For fluorescence microscopy, H1299 cells and MRC-5 cells (J. Teodoro, McGill University, Montreal, Quebec, Canada) were grown under 5% CO_2 at 37°C in media composed of DMEM (Dulbecco's Modified Eagle's Medium) and 10% Fetal Bovine Serum. Upon

reaching 80% confluency after 24 hours, the cells were transiently transfected with the constructs described above using Effectene reagent (QIAGEN, Valencia, CA) and plated in a 6-well format. These cells were concurrently transfected with CAV VP3 and GFP control.

Analysis of Sub-cellular localization

After 24 hours, the cells were fixed in 4% paraformaldehyde and PBS, and were stained with DAPI (4',6'-diamidino-2-phenylindole). Cells were mounted on slides and observed for the localization of eGFP. After 48 hours, plates of H1299 cells were observed by focusing on the center of the well under both a bright field and fluorescence in order to estimate the killing ability of PCV2a VP3 and PCV2b VP3 in comparison to CAV VP3 and the GFP control. Killing potentials were quantified by counting the number of apoptotic cells in an arbitrary quadrant of the field and extrapolating to the entire field. Bar graphs were constructed in Microsoft Excel 2003, displaying the number of apoptotic cells among all transfectants. Results were normalized by subtracting the background cell death of the GFP control from the PCV2a VP3, PCV2b VP3, and CAV VP3 transfectant samples.

3 Results

3.1 Alignment of Apoptin with PCV2 VP3 Isoforms

To determine the level of structural homology among PCV2a VP3, PCV2b VP3 and CAV VP3, we first performed an alignment of their amino acid sequences. As seen in Figure 2, PCV2b VP3 differs from PCV2a VP3 at 3 residues: a serine is substituted for a glycine at position 46; a leucine is substituted for a phenylananine at position 124; and a glutamine for a lysine at position 126. There was approximately 97% homology between both PCV2 isoforms. Analysis of functional identity among the three proteins exhibited 52% homology between both PCV2a and Apoptin, and PCV2b and Apoptin. In particular, the NES from Apoptin is relatively well conserved in both PCV2 isoforms, showing approximately 64% functional identity. In Apoptin, the NES is IRIGIAGITITLSL; in PCV2a VP3 and PCV2b VP3, it is VYI*LPITLL, where * is either glycine or serine, respectively. Visual comparison among the NLS regions of the proteins demonstrates approximately 45% functional homology. The NES regions are more conserved than the NLS in these proteins. The sequence alignment also indicated areas of homology outside of the NES and NLS domains. One amino acid of note is proline, which is conserved between PCV2 VP3 and CAV VP3 at eight positions.

3.2 Reconstruction of the Full-Length VP3 Genes and Cloning into eGFP Vector

Available clones of PCV2a VP3 and PCV2b VP3 had been linearized in the VP3 coding regions of both isoforms as seen in Figure 3. Therefore, in order to generate the full-length 2a and 2b VP3 genes, we reconstructed the VP3 coding regions using PCR. We amplified both fragments of the gene through an initial round of PCR, generating an overlapping region between

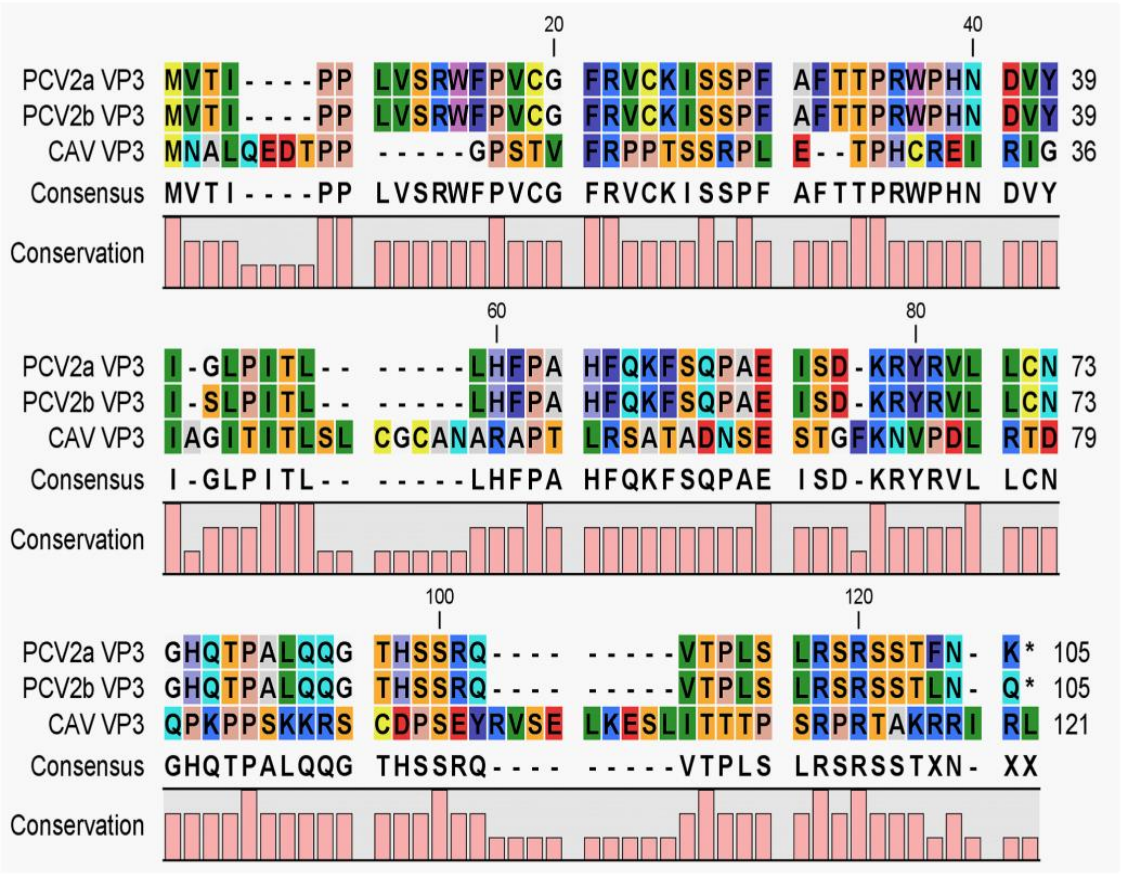

Figure 2. Amino Acid Sequence alignment (N →C) of PCV2a VP3, PCV2b VP3 and CAV VP3 (Apoptin). Apoptin's Nuclear Export Sequence can be seen from position 40 to position 59. Its Nuclear Localization Sequence can be seen at the C-terminus.

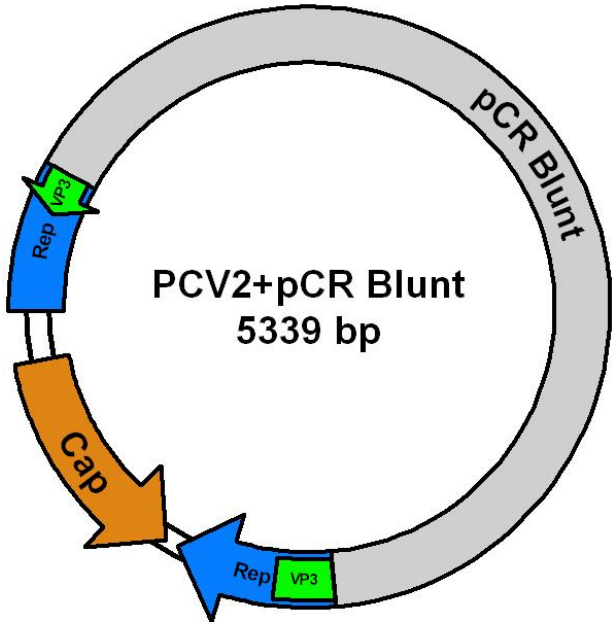

Figure 3. PCV2 Genome Cloned into PCR Blunt Vector. The available PCV2a and PCV2b clones had been linearized in the coding regions of the Rep and VP3 genes.

the fragments. We then annealed dilutions of the fragments together and through another round of PCR generated the full-length wild type VP3 genes.

The full-length 2a and 2b VP3 PCR products were then introduced into the eGFP-C1 vector through engineered BamH1 and EcoR1 restriction sites. To confirm the eGFP-VP3 constructs, the samples were restricted with BamH1 and EcoR1, as seen in Figure 4C. Additionally, sequencing analysis indicates the insertion of the VP3 genes into the vector in the correct reading frame (Figure 4D) and confirms the expected sequences for both isoforms (not shown). However the terminal amino acids for PCV2a VP3 differ from some of the PubMed sequences.

3.3 Sub-cellular Localization of the PCV2 Isotypes

After ligating the 2a and 2b VP3 genes into the eGFP vector, the constructs were transfected into H1299 and MRC-5 cells via Effectene in order to determine the sub-cellular localization patterns of the proteins. These cells were examined 24 hours after transfection. In the H1299 transformed cells, Apoptin conferred nuclear localization to GFP (see Figure 5A-C). In the MRC-5 primary cells however, Apoptin exhibited cytoplasmic localization (see Figure 5 M-O). Apoptin in particular appears punctate in both H1299 and MRC-5 cells (Figure 5B,C, N,O). Since a confocal microscope was not used to view fluorescence, expressed Apoptin-GFP appears nuclear in Figure 5N but is actually in a different plane than the nucleus. In both cell types, the GFP controls dispersed evenly throughout the cells without a distinguishable localization pattern (see Figure 5D-F and P-R). Due to the varied thickness of cells, the expression of GFP control appears more prevalent in the nuclear region (Figure 5R). The H1299 cells exhibited cytoplasmic localization for expression of both 2a VP3-GFP (Figure 5G-I) and 2b

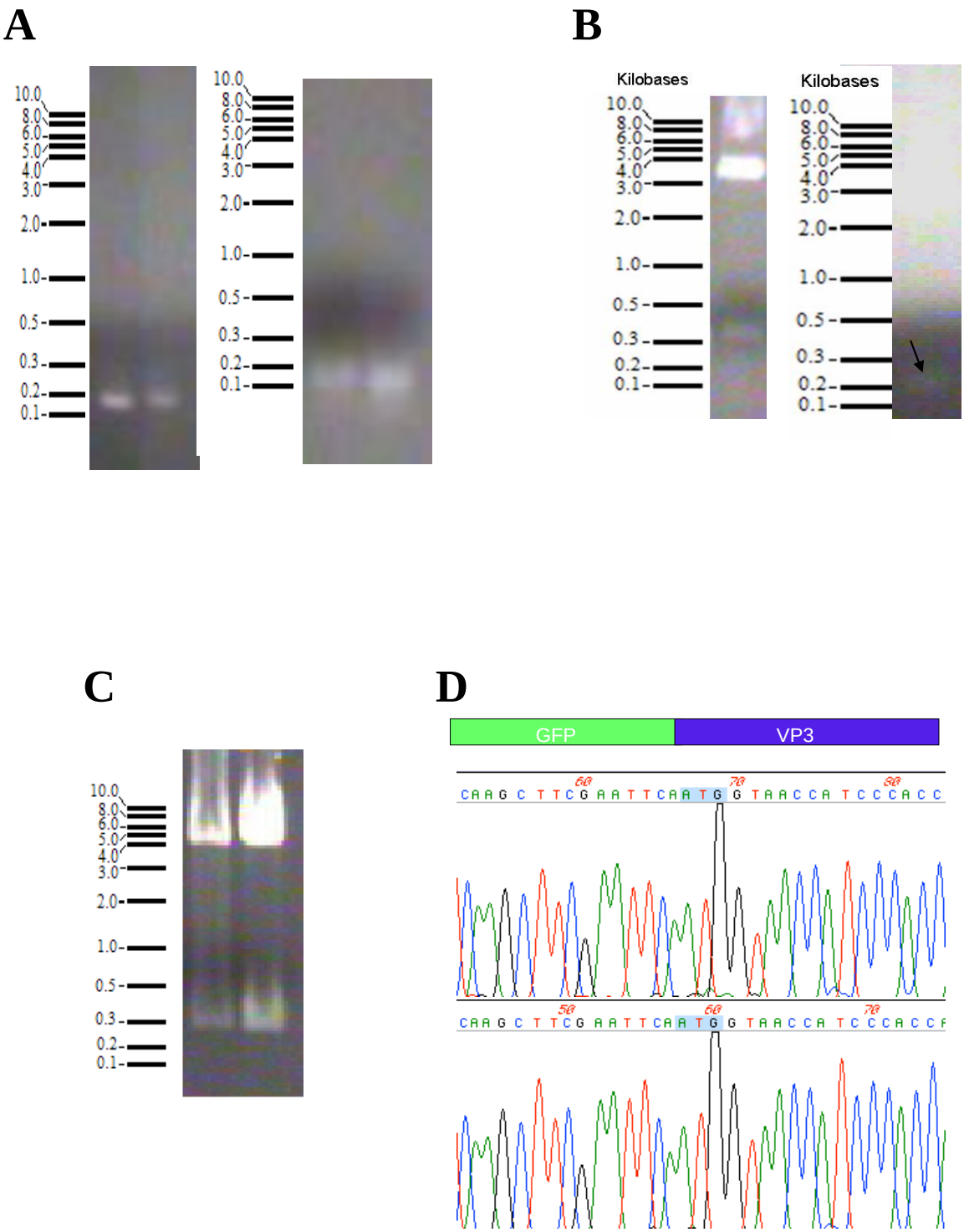

Figure 4. Reconstruction and Cloning of PCV 2 VP3. A) PCR reconstruction of full length 2a and 2b VP3. Primers were designed to amplify each fragment of the VP3 genes. The 5' and 3' fragments of 2a are shown on the left, and the 5' and 3' fragments of 2b are shown on the right. B) Subcloning of VP3 genes into T-vector. (*) C) VP3 genes (315bp) were cloned into eGFP-C1 (~4.7 kb) using BamH1 and EcoR1 restriction enzymes. D) Sequence analysis indicates a preserved open reading frame from GFP through the VP3 genes.

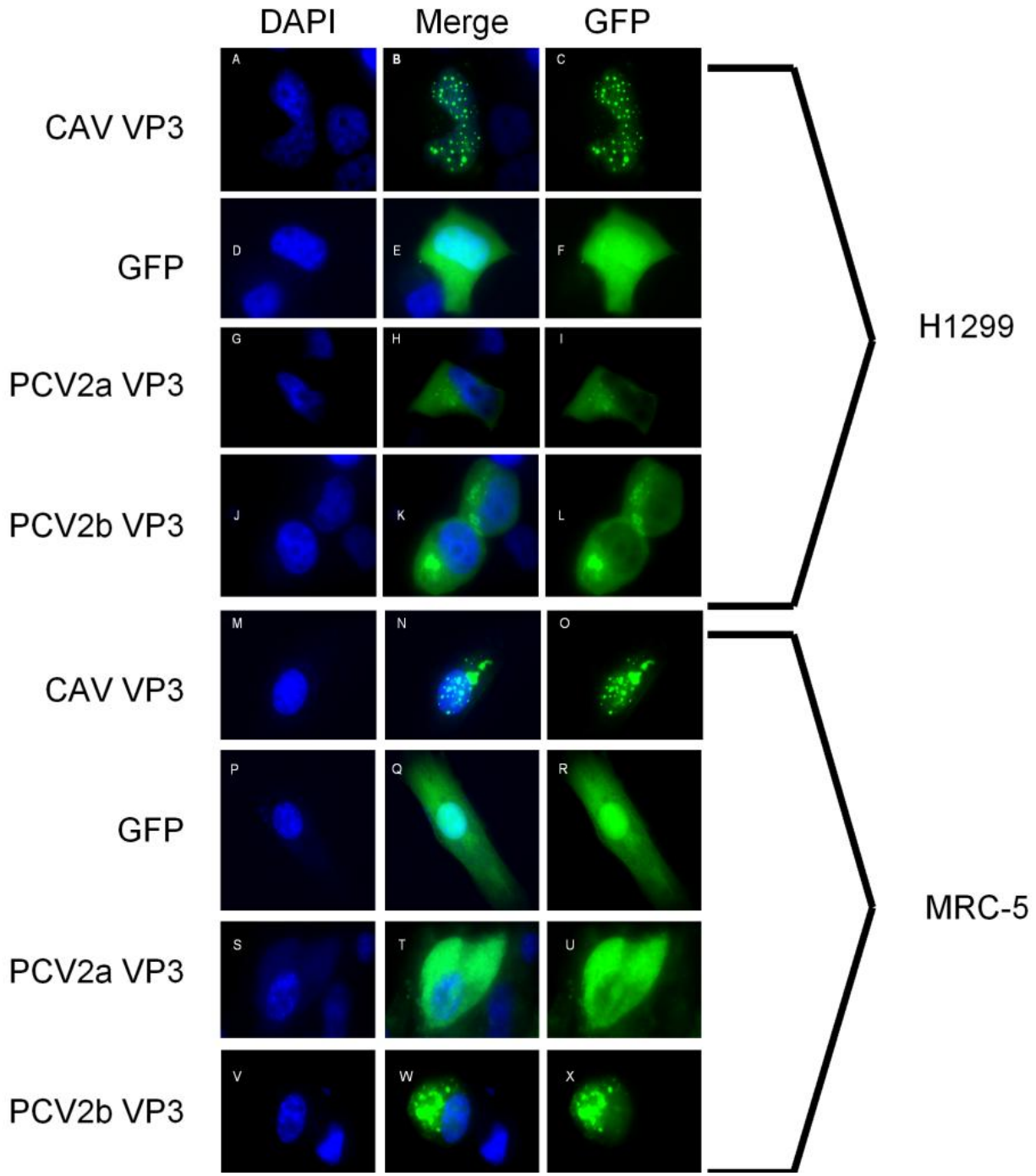

Figure 5. Localization patterns of CAV VP3, PCV2a VP3 and PCV2b VP3 in H1299 and MRC-5 cells. CAV VP3 shows nuclear localization in H1299 cells (A-C) and cytoplasmic localization in MRC-5 cells (M-O). Both PCV2a VP3 and PCV2b VP3 demonstrate cytoplasmic localization in H1299 cells (G-L) and MRC-5 cells (S-X). GFP control displays diffuse localization (D-F and P-R).

VP3-GFP (Figure 5J-L). Additionally, the MRC-5 cells displayed cytoplasmic localization patterns for 2a VP3-GFP (Figure 5S-U) and 2b VP3-GFP (Figure 5V-W).

PCV2b VP3 appears punctate in both H1299 and MRC-5 cells (Figure 5K,L,W,X) but to a lesser degree than Apoptin. PCV2a VP3 expression in H1299 appears more punctuate than the GFP control, though less than PCV2b VP3. Due to strong fluorescence, no conclusive observations can be made about the aggregation of PCV2a VP3 in MRC-5 cells (Figure 5T, U).

Finally, in order to gain a rough estimate of the killing effectiveness of PCV2a VP3 and PCV2b VP3, the transfected H1299 cells were observed in culture after 48 hours under bright field (Figure 6 A,C,E,G) and fluorescence (Figure 6 B,D,F,H) conditions. Figure 6 exhibits the H1299 cells with the apoptotic cells in focus. Figure 6A-B displays the H1299 cells transfected with Apoptin and Figure 6C-Dshows those transfected with a GFP control. The cells expressing PCV2a VP3 and PCV2b VP3 are depicted in Figure 6E-F and G-H, respectively. Upon analysis of these images, it can be noted that there is a greater amount of apoptotic cells in the PCV2a, PCV2b, and CAV VP3 samples than in the GFP control sample.

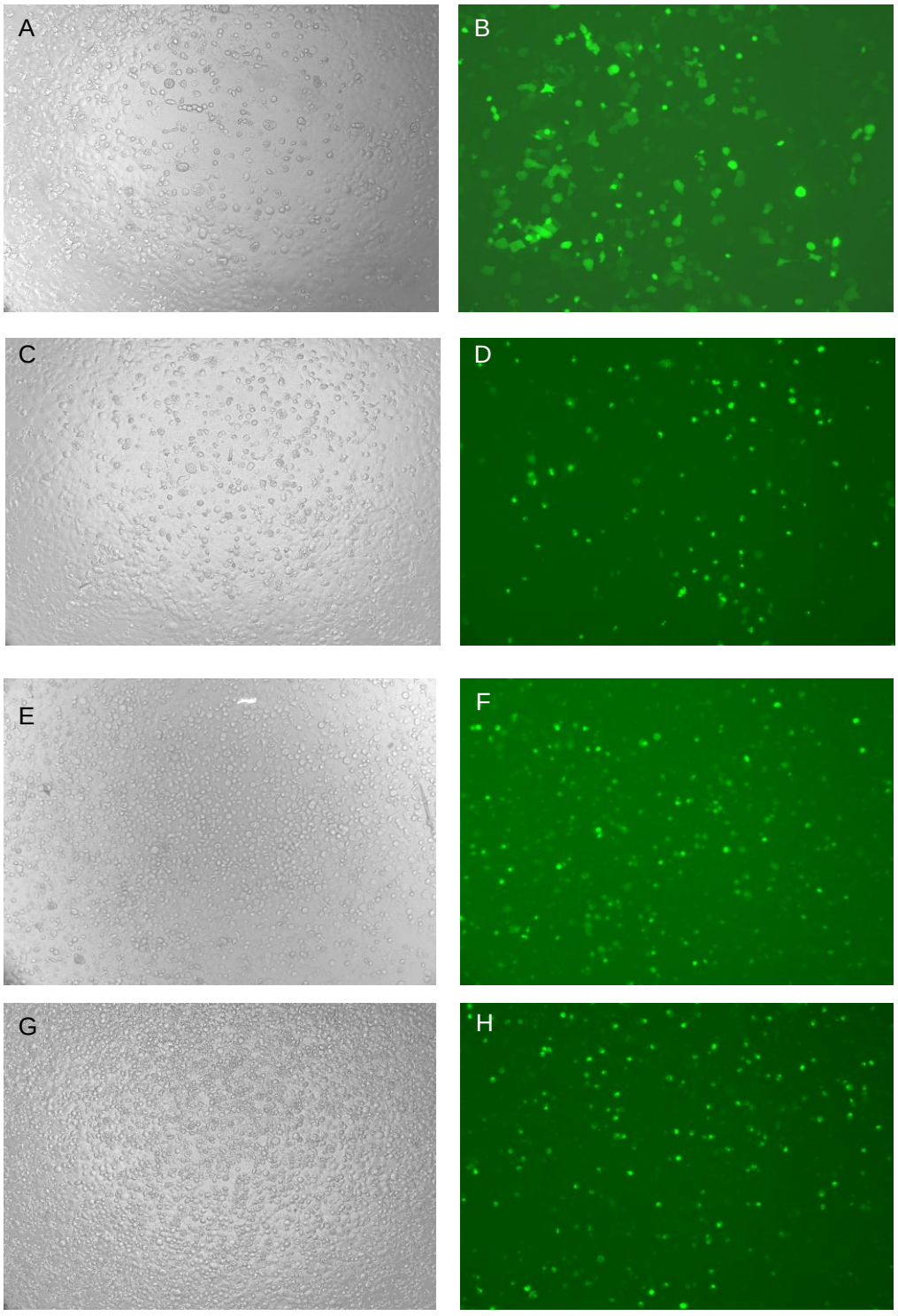

Figure 6. 20X magnification of H1299 cells 48 hours after Transfection. Fluorescence indicates GFP positive cells. The bright field view is focused on apoptotic cells. The field of view for PCV2a VP3 (E-F), PCV2b VP3 (G-H), and CAV VP3 (A-B) contain more apoptotic cells than the GFP control (C-D).

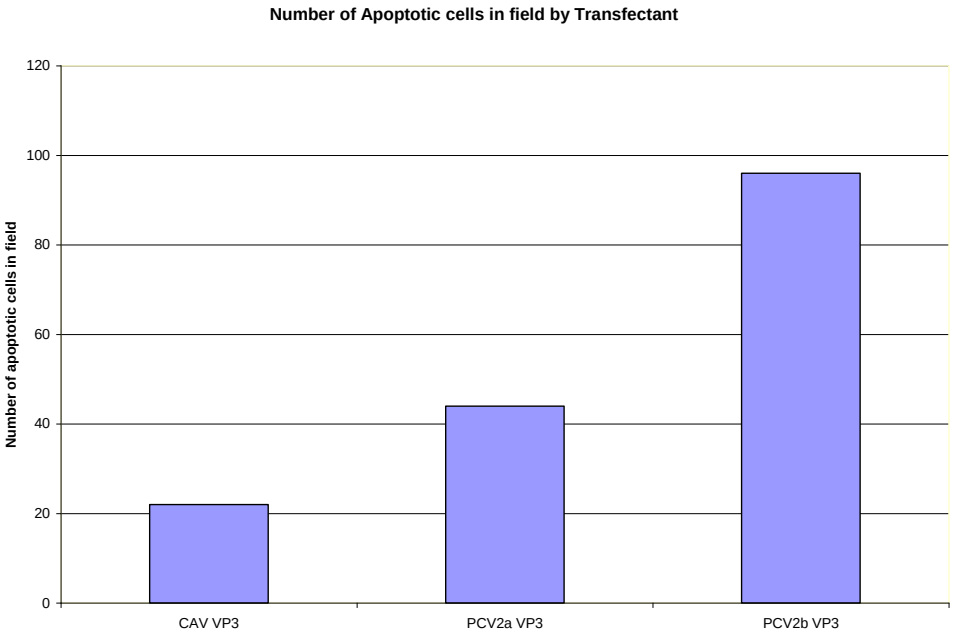

Figure 7. Quantitative Analysis of Apoptosis in H1299 Cells. The data was normalized based on GFP control for basal cell death.

4 Discussion

The sub-cellular localization patterns of Apoptin are believed to be involved in transformed cell-specific apoptosis. Previous studies have indicated that PCV2 VP3 is required for viral pathogenesis, which is linked to the induction of apoptosis. Both PCV2 and CAV are of the *Circovidae* family, and encode for viral proteins involved in the induction of apoptosis. Although PCV2 is known to cause cell death in pigs, the localization patterns of PCV2a VP3 and PCV2b VP3 in both primary and transformed cells had yet to be determined. Since Apoptin exhibits transformed cell specific activities, we have taken the opportunity to investigate PCV2a VP3 and PCV2b VP3 in the same context.

As part of our analysis, we evaluated the level of homology among PCV2a VP3, PCV2b VP3 and Apoptin in order to determine the differences among the proteins at the amino acid level. A bulk of the work focused on producing wild-type genes for PCV2a and PCV2b VP3 via PCR reconstruction. These genes were sub-cloned into a T-vector, and subsequently cloned into eGFP-C1. We developed these constructs to fuse GFP to the N-terminus of both PCV2a VP3 and PCV2b VP3 to allow visualization of protein expression and characteristics of sub-cellular localization. To view these properties in transformed cells, we transfected H1299 cells, which are P53 null human lung cancer cells. We performed the same analysis in MRC-5 cells, which are normal, primary, human muscle fibroblasts.

According to the alignment of the PCV2a VP3 and PCV2b VP3 amino acid sequences with Apoptin, there is a high degree of homology among the proteins, approximately 52%. In particular, the NES remains highly conserved among the three viral proteins with a functional identity of 64%. Conversely, the NLS of both 2a and 2b VP3 are more divergent from that of Apoptin demonstrating 45% functional identity. In addition to the homology in both the NLS

and NES, other conserved amino acids are noteworthy. Among these is proline which recurs eight times at similar locations in all three proteins. There are five of these prolines to the N-terminal side of the NES, one between the NES and the NLS, and two within the NLS. These may be significant in prediction of both the secondary and tertiary structures of the proteins, because they tend to disrupt α-helices and β-sheets. Regions other than the NLS and NES also exhibit high functional conservation, indicating that these regions may generate domains of similar function. It would be expected that the NES of PCV2 would be functional and active under the same conditions as Apoptin, thus conferring cytoplasmic localization in normal primary cells. Due to a lesser degree of homology within the NLS of Apoptin, no conclusion can be reached concerning the nuclear localization of PCV2 VP3.

Next, in order to analyze the functions of PCV2a VP3 and PCV2b VP3, we needed to generate the full length genes for both proteins. Since the clones we received had been linearized within ORF3 (Figure 3), it was necessary to reconstruct both genes. We designed primers, seen in Tables 1 and 2, to amplify both fragments of each VP3 gene. These primers included regions of overlap at the interior of the gene in order to facilitate annealing for the final PCR reconstruction. The terminal primers contained restriction sites for EcoR1 and BamH1 at the 5' and 3' ends respectively. Analysis through agarose gel electrophoresis indicated that both fragments of each gene were properly amplified. As seen in Figure 4A, both fragments of each gene are approximately the same size. We successfully annealed these fragments together and generated a wild-type copy of each gene through a final round of PCR.

Upon analysis with fluorescence microscopy, the sub-cellular localization patterns of the VP3 constructs samples were determined. CAV VP3 exhibited nuclear localization in H1299 cells as seen in Figure 5A-C. In MRC-5 cells however, CAV VP3 localized in the cytoplasm as

seen in Figure 5M-O. Although Figure 5N may suggest mixed localization patterns, a confocal microscope was not used in data collection, and the expressed GFP was therefore not in the plane of the nucleus. These localization patterns are consistent with published data on the localization trends of Apoptin in various cell types. It is also known that the cytoplasmic localization of Apoptin is dependent on the exportin CRM1. These distinct localization patterns may occur for a number of different reasons. For example, since nuclear transport receptors are up-regulated in transformed cells, nuclear localization may occur due to an increased concentration of importins. Alternatively, post-translational modifications of Apoptin may be necessary for nuclear localization in transformed cells. This modification may make the NLS of the protein more accessible to transport receptors than the NES, therefore favoring its import into the nucleus.

These experiments also confirmed that both PCV2a VP3 and PCV2b VP3 have a functional NES. If the proteins did not contain a functional NES, they would be expected to display a localization pattern similar to that of the GFP control (Figure 5D-F and P-R), in which the protein would disperse evenly throughout the cell. As seen in Figure 5G-L both proteins exhibit cytoplasmic localization in H1299 transformed cells. The proteins also demonstrated cytoplasmic localization in normal MRC-5 primary cells. The NES of both PCV2 VP3 isoforms are about 64% homologous with that of Apoptin and are rich in leucines and isoleucines, thus making the PCV2 VP3s prime targets for export by CRM1.

Despite similar localization patterns in normal primary cells among the three proteins, Apoptin exhibits nuclear localization in transformed cells, whereas PCV2a VP3 and PCV2b VP3 localize in the cytoplasm. A number of possibilities concerning the properties of the NLS can be drawn from this result. First, the NLS of the PCV2 VP3s may not be functional. To examine this hypothesis, the NLS alone from these proteins could be fused to GFP. This analysis could

yield two different results: nuclear localization or diffuse localization. If the NLS is functional in the above experiment, the protein should localize in the nucleus due to the absence of an NES. Conversely, if the NLS is non-functional, the protein should not localize in a particular sub-cellular compartment. To achieve these results, transfections should be performed similar to those in this study. Sub-cellular localization should be analyzed both before and after treatment with Leptomycin-B in order to determine if PCV2 VP3 participates in nucleocytoplasmic shuttling. This would indicate whether the NLS is active under normal conditions by nuclear localization of the proteins in both normal, primary cells and transformed cells. Additionally one could attach the functional NLS from Apoptin to PCV2 VP3 to see if it alters cellular localization in both cell types. If a change in localization patterns is observed, killing experiments could determine if this results in the gain of cell type specificity.

Fluorescence microscopy analysis yielded interesting results in addition to the localization patterns of the proteins. For example, in both H1299 and MRC-5 cells CAV VP3 displays a punctate phenotype, a pattern which is not as strong in PVC VP3 samples. PCV2a VP3 appears slightly punctate in H1299 cells, and PCV2b VP3 appears slightly punctuate in both cell types. The expression of GFP in PCV2a VP3 transfected MRC-5 cells is too strong, thus preventing analysis of its clustering properties. These data may suggest that PCV2a VP3 and PCV2b VP3 may multimerize in vivo, though to a lesser degree than Apoptin. Multimerization, therefore may be involved in the cell type specific activities of Apoptin. Another factor resulting in the punctate appearance of the proteins is their fusion to GFP. Due to its size, GPF disrupts the otherwise filamentous multimerization pattern of Apoptin. The fusion of PCV2a VP3 and PCV2b VP3 to GFP may also be a factor in their punctuate appearance. Similar to Apoptin, these proteins may multimerize in vivo. To test this possibility, immunolocalization

experiments may be performed in order to further evaluate the multimerization effects of PCV2a VP3 and PCV2b VP3 without the interference of GFP.

Due to the unique localization patterns of PCV2a VP3 and PCV2b VP3 in relation to Apoptin, we then examined the killing potential of the proteins 48 hours after transfection. This analysis was performed under both a bright field and fluorescence to detect the presence of GFP. Only H1299 cells were examined due to poor transfection efficiency with the MRC-5 primary cells. Analysis of the killing experiments indicates that H1299 cells transfected with Apoptin, 2a VP3 and 2b VP3 displayed a higher mortality rate than those transfected with the GFP control. Rough estimates of VP3 induced cell death were formed by examining Figures 6A, C, E, and G. Figures 6B, D, F, and H indicate that a number of cells in focus are expressing GFP.

Next, we performed a semi-quantitative analysis of the level of apoptosis induced by each transfectant by counting the number of apoptotic cells in one quadrant of the field. The resulting graph seen in Figure 7 displays the number of apoptotic cells for the CAV VP3, PCV2a VP3 and PCV2b VP3 transfectants with a baseline correction for the GFP control. Since GFP alone can not independently induce apoptosis, it is a good measure for the level of background cell death. As seen in Figure 7, CAV VP3 produced approximately 20 apoptotic cells above the baseline; PCV2a VP3 produced approximately 40 apoptotic cells; and PCV2b VP3 produced approximately 100 apoptotic cells. The observations in Figure 7 suggest that PCV2b VP3 induces apoptosis in a greater number of transformed cells than PCV2a VP3. This variance may be related to varied transfection efficiencies or to an inherent level of killing capability. If the latter is true, the increased killing efficiency of PCV2b VP3 may be attributed to one or more of the amino acids distinct from the PCV2a VP3 sequence. Further investigation should use flow cytometry to accurately quantify the number of apoptotic cells resulting from each transfectant.

This analysis should be performed for both H1299 cells and MRC-5 cells granted that sufficient transfection rates can be obtained. Killing analysis in MRC-5 cells could indicate one of many possibilities. First, PCV2 VP3 could function like Apoptin and not induce apoptosis within primary cells. If this were the case, sub-cellular localization would not be required for transformed cell-type specific induced apoptosis. Second, PCV2 VP3 could induce apoptosis in primary cells. Since both PCV2 proteins induce cell death while exhibiting cytoplasmic localization in transformed cells, they may also be able to stimulate apoptosis in primary cells, in which they show the same localization pattern.

The results of this study have several implications for PCV2 VP3 and its homolog, CAV VP3. First, differences in the sub-cellular localization patterns may indicate a unique mechanism of action for each protein. Despite the cytoplasmic localization of PCV2a VP3 and PCV2b VP3, these proteins exhibit a similar apoptotic phenotype to Apoptin in transformed cells. Previous studies have indicated that nuclear localization of Apoptin plays a significant role in the induction of apoptosis, which is linked to an interaction with the APC in the nucleus. One possible mechanism is that the PCV2 proteins interact with a cytoplasmic target. Cytoplasmic APC is a plausible target because a number of nuclear proteins are regulated by their export into the cytoplasm. In fact, the APC has been found in the cytoplasm of neurons. P53 is not involved in the apoptotic pathway of PCV2 VP3 because cell death was induced in H1299 cells, which are P53 null. Thus, if Pirh2 E3 ligase is the target of PCV2 VP3, it must act independently of P53.

Another possibility is that the PCV2 proteins function similarly to Apoptin, except that they gain access to the contents of the nucleus during its breakdown in cell division. This mechanism is supported by the phenotype of PMWS. The cell types primarily affected by this

disorder include dermal, lung, and intestinal cells. Each of these cell types divides regularly and thus would be a prime target for VP3 induced apoptosis due to mitotic nuclear breakdown.

Further experimentation with PCV2a VP3 and PCV2b VP3 may shed some light on Apoptin's role in cell type specific apoptosis. First, quantitative analysis of VP3 induced cell death should be performed via flow cytometry in order to determine if PCV 2a VP3 or PCV2b VP3 demonstrate unique killing potentials. This analysis would also be able to detect a possible difference between the killing potentials of PCV2 VP3 in transformed and primary cells. Additionally, the level of sub-cellular localization should be evaluated using fluorescence quantification software. Next, it should be determined if 2a and 2b VP3 demonstrate distinct phenotypes in primary and transformed cells.

Another worthwhile experiment would be to generate truncation mutants of the full length VP3 gene in order to analyze the functional characteristics of each mutant within both transformed and primary cells. This analysis would investigate the influence of the different domains of PCV2 VP3 on its sub-cellular localization patterns. Furthermore, the killing potentials of each truncation mutant may be evaluated and compared with one another in order to map the binding domains for target molecules within the full length protein. Other areas of interest include investigation of PCV2 VP3 multimerization characteristics and determination of its molecular target. These studies would involve yeast two-hybrid experiments to examine the multimerization capabilities of PCV2a VP3 and PCV2b VP3. Moreover, the affinity for potential target molecules (e.g. APC, Pirh2) could be assessed using the same system. Analysis of PCV2a VP3 and PCV2b VP3 may help to elucidate Apoptin's mechanism of action and could provide further insight into transformed cell specific activities.

References

1. **Bratanich, A.C. and A. Blanchetot.** 2002. PCV2 Replicase Transcripts in Infected Porcine Kidney (PK 15) Cells. *Virus Genes.* **25:** 323-328.

2. **Budihardjo, I., Oliver, H., Lutter, M., Luo, X. and Wang, X.** 1999. Biochemical Pathways of Caspase Activation During Apoptosis. *Annu. Rev. Cell Dev. Biol.* **15**: 269-290.

3. **Danen-Van Oorscht, A.A., D.F. Fischer, J.M. Grimbergen, B. Klein, S. Zhuang, J.H. Falkenburg, C. Backendorf, P.H. Quax, A.J. Van der Eb and M.H. Noteborn.** 1997. Apoptin Induces Apoptosis in Human Transformed and Malignant Cells but not in Normal Cells. *Proc. Natl. Acad. Sci.* **94:** 5843-5847.

4. **Fenaux, M., Opriessnig, T., Halbur, P.G., and X. J. Meng.** 2003. Immunogenicity and Pathogenicity of Chimeric Infectious DNA Clones of Pathogenic Porcine Circovirus Type 2 (PCV2) and Nonpathogenic PCV1 in Weanling Pigs. *Journal of Virology.* **77**: 11232-11243.

5. **Fornerod, M., Ohno, M., Yoshida, M., and Mattaj, I**. 1997. CRM1 is and Export Receptor for Leucine-Rich Nuclear Export Signals. *Cell.* **90**:1051-1060.

6. **Gagnon, C.A., D. Tremblay, P. Tijssen, M.H. Venne, A. Houde, and S. M. Elahi**. 2007. The emergence of porcine circovirus 2b genotype (PCV-2b) in swine in Canada. *Can Vet J.* **48**(10): 811–819.

7. **Harper, W. J., J.L. Burton, M.J. Solomon.** 2002. The anaphase-promoting complex: it's not just for mitosis any more. *Genes&Dev.* **16**: 2179-2206.

8. **Heilman, D.W, M.R. Green and J.G. Teodoro.** 2005. The Anaphase Promoting Complex. *Cell Cycle.* **4:** 560-563.

9. **Heilman, D.W., J.G. Teodoro and M.R. Green.** 2006. Apoptin Nucleocytoplasmic Shuttling is Required for Cell Type-Specific Localization, Apoptosis, and Recruitment of the Anaphase-Promoting Complex/Cyclosome to PML Bodies. *J. Virol.* **80:** 7535-7545.

10. **Liu, Jue Chen, Isabelle, and Kwang, Jimmy**. 2005. Characterization of a Previously Unidentified Viral Protein in Porcine Circovirus Type 2-Infected Cells and Its Role in Virus-Induced Apoptosis. *J. Virol.* **79:** 8262–8274.

11. **Liu, Jue, Chen, Isabelle, Du, Qingyun, Chua, Huikheng, and Kwang, Jimmy.** 2006. The ORF3 Protein of Porcine Circovirus Type 2 Is Involved in Viral Pathogenesis In Vivo. *J. Virol.* **80:** 5065-5073.

12. **Liu, J., Y. Zhu, I. Chen, J. Lau, F. He, A. Lau, Z. Wang, A.K. Karuppannan, and J. Kwang.** 2007. The ORF3 Protein of Porcine Circovirus Type 2 Interacts with Porcine Ubiquitin E3 Ligase Pirh2 and Facilitates p53 Expression in Viral Infection. *J. Virol.* **81:** 9560-9567.

13. **Mankertz, A., Mankertz, J., Wolf, K. and H.J. Buhk.** 1998. Identification of a Protein Essential for Replication of Porcine Circovirus. *Journal of General Virology.* **79:** 381-384.

14. **Mankertz, J., Buhk, H.J., Blaess, G. and A. Mankertz.** 1998. Transcription Analysis of Porcine Circovirus (PCV). *Virus Genes.* **16:** 267-276.

15. **Morgan, D.** 1999. Regulation of the APC and the Exit from Mitosis. *Nature Cell Biology.* **1:** E47-E53.

16. **Nakielny, S., and Dreyfuss, G.** 1999 Transport of Proteins and RNAs in and out of the Nucleus. *Cell.* **99**:677-690.

17. **Peters, J.M.** 2002. The anaphase-promoting complex: proteolysis in mitosis and beyond. *Mol. Cell* **9:** 931-943.

18. **Rustgi, A.** 2002. Securin a New Role for Itself. *Nat. Genet.* **32**, 222-224.

19. **Teodoro, J.G., D.W. Heilman, A.E. Parker and M.R. Green.** 2004. The Viral Protein Apoptin Associates with the Anaphase-Promoting Complex to Induce G2/M arrest and Apoptosis in the Absence of p53. *Genes & Development.* **18:** 1952-1957.

20. **Terry, L., Shows, E., and Wente, S**. 2007 Crossing the Nuclear Envelope: Hierarchical Regulation of Nucleocytoplasmic Transport. *Science.* **318**: 1412-1416.

21. **Timmusk, S., Fossum, C. and M. Berg.** 2006. Porcine Circovirus type 2 Replicase Binds the Capsid Protein and an Intermediate Filament-like Protein. *Journal of General Virology.* **87:** 3215-3223.